Validation of a Pyrolysis Model of Wood Thermal Decomposition under Cone Calorimeter

Colombiano J.[1,2,]*, Dréan V.[1], Rogaume T.[2], Richard F.[2], Batiot B.[2], Fateh T.[3], Nadjai A.[4], Guillaume E.[1]

[1] *Efectis France, France*
[2] *Instit Pprime/UPR3346 CNRS, Université de Poitiers, ISAE-ENSMA, France*
[3] *Efectis UK, Nothern Ireland*
[4] *Fire SERT, Ulster University, Northern Ireland*
**Corresponding author's email: jeremy.colombiano@efectis.com*

ABSTRACT

In this paper, the thermal decomposition of wood is investigated. The multi-scale approach followed here allows first to establish, at a small scale, the kinetic mechanism during the solid thermal decomposition and then validate it at a larger scale. At small scale, experiments were conducted by using Thermo-gravimetric analysis (TGA). Thermo-gravimetric results were also used to propose a kinetic mechanism for the thermal decomposition of the sample. The kinetic parameters of the different identified reactions were estimated by using an optimization technique, namely the Particle Swarms Optimization (PSO) method. The mass loss and mass loss rate model predictions show a good agreement with the experimental data. In addition, heat capacity, as well as heat of reaction, is determined using a TGA-DSC (Differential scanning calorimetry) apparatus.

At a larger scale, experiments were carried out in a cone calorimeter under air atmosphere. The sample is placed in an insulated sample holder (calcium silicate). The pyrolysis model developed at the TGA scale and the measured thermal parameters were used in numerical simulations of cone calorimeter experiments taking into account the modelling of heat transfer into the sample.

The comparison between experimental and numerical results under cone calorimeter is made on the mass loss, the mass loss rate, the temperatures and the pyrolysis front. The numerical results can predict the thermal behavior. The noted differences are mainly due to a lack of control of the experimental boundary condition, and are also partly attributable to the evaporation of water present in the sample holder which is not taken into account.

KEYWORDS: Thermal degradation, cone calorimeter, TGA, Fire Dynamics Simulator.

NOMENCLATURE

A	pre exponential factor (s^{-1})
E	Activation energy (kJ/kmol)
c_P	constant pressure specific heat (J/(kg·K))
q''	heat flux (W/m^2)
q'''	heat release rate (W/m^3)
n	reaction order
R	ideal gas constant value (kJ/(kmol·K))
T	temperature (K)
λ	thermal conductivity (W/(K·m))
ρ	density (kg/m^3)
ω	reaction rate (s^{-1})

Subscripts

0	initial
c	chemical
r	radiative
s	solid phase

Proceedings of the Ninth International Seminar on Fire and Explosion Hazards (ISFEH9), pp. 1053-1065
Edited by Snegirev A., Liu N.A., Tamanini F., Bradley D., Molkov V., and Chaumeix N.
Published by Saint-Petersburg Polytechnic University Press
ISBN: 978-5-7422-6498-9 DOI: 10.18720/spbpu/2/k19-87

t time (s)

Greek

ε emissivity (-)

g gas phase

i reaction number

INTRODUCTION

The equations of motion describing the gas phase in Computational Fluid Dynamics (CFD) are relatively well known and the approximations in the various gas phase sub-models have been extensively studied. However, the coupling between the gas phase and the condensed phase in order to describe flame spread over a burning solid has proven difficult to model. Due to lack of knowledge on the underlying phenomena during the decomposition of the solid, the poor characterization of the fundamental material properties that controls the burning process and the large assumption of wall submodels, fire ignition and propagation cannot be accurately predicted, taking into account a mechanism of decomposition [1, 2]. Some studies have been focused on fire ignition and propagation at large scales, but empirical laws are used, such as the definition of an ignition temperature and the prescription of a mass flow of pyrolysis versus time [3]. Other models avoided the use of an ignition temperature and described the ignition by a critical mass loss rate [4]. However, a detailed analysis of thermal decomposition was still avoided. Describing the material behavior for fire prediction is a key challenge for the fire community.

Therefore, it is of the first importance to determinate material parameters and to identify the physical and chemical phenomena involved in order to numerically predict the material behavior for prediction of fire dynamics. The goal of this study is to improve the capability of the fire model (e.g. Fire Dynamics Simulator [5]) to predict flame spread over materials that burn in a scale like compartment fire, by taking material behavior into account. This report is only focused on the TGA and cone calorimeter scale results.

There is a substantial volume of work in the literature regarding the material behavior and the transition between the TGA scales to the cone calorimeter. Bustamante studied the thermal decomposition of polyether polyurethane foam [6] and used for the first time the multi-scale approach. Since then, studies using this approach are mainly focused on the mass loss, mass loss rate and heat release rate prediction [7, 8]. Others studies attempted to numerically predict the temperature of the sample. But, as it is shown by Fateh [9], the prediction of the mass loss, the mass loss rate and the temperatures does not mean that the pyrolysis front is correctly predicted. Fateh [9] studied a multi-scale approach for plywood. The thermal decomposition model proposed in his study is composed of five reactions, taking into account oxygen effect. The thermal parameters are estimated based on the mass loss rate of the cone calorimeter experimental result. The numerical prediction for the mass loss, mass loss rate and temperatures (at the surface and bottom of the sample) are in good agreement with the experimental results, but the pyrolysis front is not correctly tracked.

This paper is focused on the prediction of the material behavior of fir wood under cone calorimeter. Wood constitutes a substantial fraction of the fuel load in building fires. For this reason, understanding of its behavior under high temperature conditions is important. Wood is a charring fuel and undergoes a variety of complex physical and chemical processes of momentum, heat and mass transfer, property variations, structural changes, char oxidation and secondary chemical reactions within the solid [10]. Oxygen concentration, irradiance, moisture content and the orientation of the solid fuel with respect to the external heat source affect the pyrolysis process (e.g. flames). TGA, TGA-DSC are used to determinate a model of thermal decomposition, heat capacity and heat of reaction. These parameters serve as input data for the prediction of the material behavior

under cone calorimeter for different heat fluxes. Comparisons of numerical and experimental mass loss, mass loss rate, temperatures and pyrolysis front are presented.

THERMOGRAVIMETRIC ANALYSIS

The first part of this work intends to develop a pyrolysis model. An experimental investigation has then been conducted at matter scale in order to define the mechanism of thermal decomposition. The kinetic parameters associated have been calculated.

A Mettler TGA-DSC apparatus was used to study the decomposition kinetics of the sample. The furnace was heated at a constant heating rate (5 K/min) and experiments were performed under nitrogen and air, in order to separate the thermolysis and oxidative reactions. Using a small heating rate allow us to avoid temperature gradient and mass diffusion in the sample. For the same reason, the polymers were cut into thin samples of 0.3 mm high and 5 mm diameter, for a mass of 6 ± 2 mg. Thus, the temperature in the sample was assumed to be same as that of the sample compartment. The furnace was continuously purged with $5 \cdot 10^{-7}$ m^3/s of ultra-high purity nitrogen or air. Figure 1 presents the TGA experimental results as a function of temperature in inert and air atmosphere.

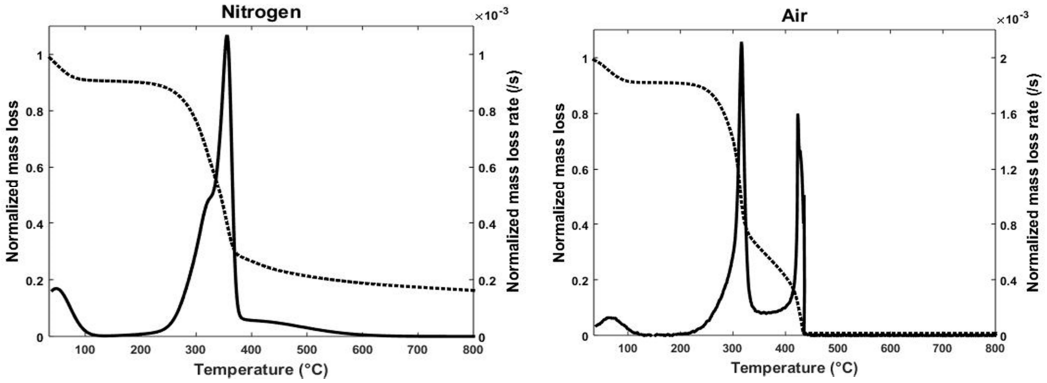

Fig. 1. TGA experimental results of wood decomposition under nitrogen (a) and air (b) at 5 K/min.

After the water evaporation (up to 100°C), independently of the heating rate, the wood thermal degradation begins at 200°C up to around 600°C and leads to a residue of around 0.18 for nitrogen atmosphere. The results obtained are in accordance with the literature [10]. Indeed, several studies have been focused on the kinetic mechanism of the thermal decomposition of the wood and show that it begins to degrade with the hemicellulose, from 200 and 325°C. Then cellulose starts its degradation from 240 to 375°C, and lignin from 250 to 600°C [10]. In air atmosphere, wood degrades at around 300°C, and char oxidation takes places at 430°C, leading to no residue.

The thermal decomposition mechanism proposed here represents these degradations (hemicellulose, cellulose and lignin) by one reaction only. The decomposition mechanism is obtained from the coupled analysis of the curves of mass loss and mass loss rate, using a Lumped parameter approach (LPA). The model is composed of three reactions including the water evaporation:

$$\begin{aligned} &Wet\ wood \xrightarrow{N2} Dry\ wood + Water\ vapor \\ &Dry\ wood \xrightarrow{N2} Char\ wood + Gas \\ &Char\ wood \xrightarrow{Air} Residue + Carbon\ dioxide \end{aligned} \quad . \tag{1}$$

Oxygen effect is taken into account by the third reaction. In fact, it is assumed that there is no oxidation reaction in the sample at the cone calorimeter. Indeed, at the cone calorimeter scale, it is assumed that the pyrolysis flow avoids oxygen diffusion in the sample. In addition, at the surface of the sample, oxygen is practically consumed by oxidation reactions. This assumption is particularly true for high incident heat fluxes [10, 11]. Therefore, char oxidation is taken into account only for the surface of the sample.

Each reaction *i* is characterized by its reaction rate, defined as:

$$\dot{\omega}_i = A_i \exp\left(-\frac{E_i}{RT}\right) Y_{S,i}^{n} Y_{O_2,i}^{n_{O_2}}, \tag{2}$$

where A_i is the pre-exponential factor of the reaction *i*, E_i is the activation energy, $Y_{S,i}$ and $Y_{O_2,i}$ are, respectively, the mass fraction of the combustible and air, n and n_{O_2} expressing the order of each reagent.

The set of kinetic parameters of each reaction is determined using the heating rate of 5 K.min^{-1} to keep the assumption of no gradient of mass and temperature. The parameters are estimated using an inverse optimization method based on a modelistic approach (the parameters are constant for each reaction), here the particle swarm algorithm is used and its performance has already been demonstrated [12]. For more information about this algorithm, see [13]. Only the mass fractions of the generated species are estimated experimentally (with the mass loss curves). The set of kinetic parameters are presented in the Table 1. Figure 2 presents the mass loss rate for nitrogen and air obtain by the model, in comparison with the experimental results.

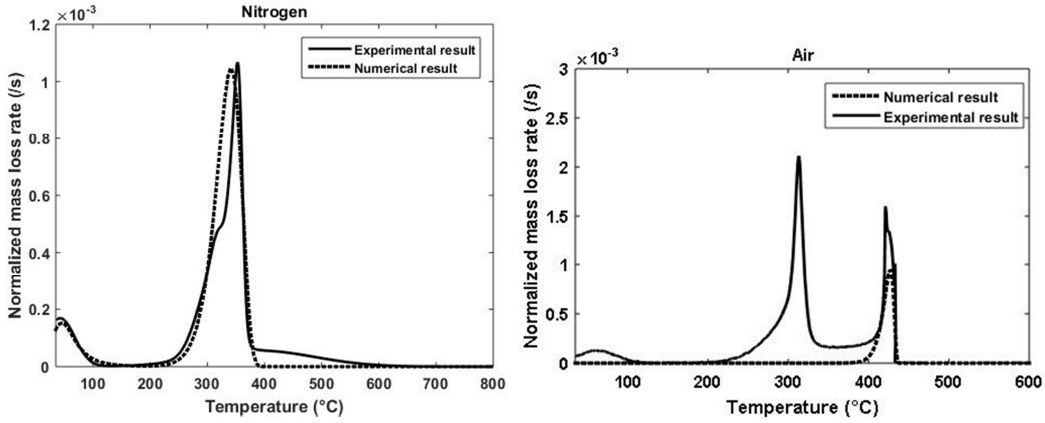

(a) (b)

Fig. 2. Experimental and numerical TGA results at 5K/min under nitrogen (a) and air (b).

It can be seen from Fig. 2(b) that the mass loss rate of the char oxidation is not correctly represented. This is due to the inability of the model to predict brutal reactions as char. Once the reactions and associated parameters of the condensed phase are identified, the pyrolysis model can be used to predict the thermal decomposition under cone calorimeter scale. Therefore, the thermal properties of the wood have to be determined. The Differential Scanning Calorimetric (DSC) apparatus is used for the characterization of the heat capacity of the wood and the char. No distinction between hemicellulose, cellulose and lignin is made, as the thermal mechanism used a LPA approach. The heat of reaction is also determined for each reaction, according to [14, 15]. The thermal conductivity of the wet wood is evaluated from measurements at room temperature with a

Modified Transient Plane Source (MTPS) Technique. Thermal conductivities of dry wood and char are chosen from the reference [16]. The density of the wet wood is directly measured, and the densities of dry wood and char are estimated according to [16]. Table 1 shows the parameters used in the simulation, the heat capacity is given here at room temperature, and the emissivity is equal to 1 for all materials [17].

Table 1. Kinetic parameters for the LPA model of decomposition

	A, s^{-1}	E, kJ/kmol	υ	n	n_{O2}	ρ, kg/m^3	λ, W/(m·K)	C_p, kJ/(kg·K)
Wet wood	4.06E8	6.7E4	0.9	2.8	0	447	0.13	1.39
Dry wood	1.59E9	1.37E5	0.2	1.36	0	410 [16]	[16]	1.39
Char	1.86E24	3.5E5	0	0.5	1	130 [16]	[16]	1.04

CONE CALORIMETER EXPERIMENTAL RESULTS

In order to validate the model of pyrolysis and the thermal parameters, tests using the cone calorimeter apparatus are performed. Then, comparisons of experimental and numerical mass loss, mass loss rate, temperatures and pyrolysis front are presented.

The sample is placed in the horizontal position in an insulated sample holder limiting the thermal transfer at the side and back of the sample. Heat and mass transfers are then assumed to be in one dimension (perpendicular to the surface exposed). A flame development appears at this scale.

The experiments are conducted under air atmosphere, with well-ventilated conditions and with a piloted ignition. The heat fluxes studied are 20, 30, and 50 kW/m^2. The size of the sample is 100×100×18 mm^3 and its mass is about 78g (± 6g). Figure 3 summarizes the evolution of the normalized mass loss and the normalized mass loss rate. The mass loss rate curves are obtained by first applying a Savitzky Golay filter, and then by fitting with Gaussian curves.

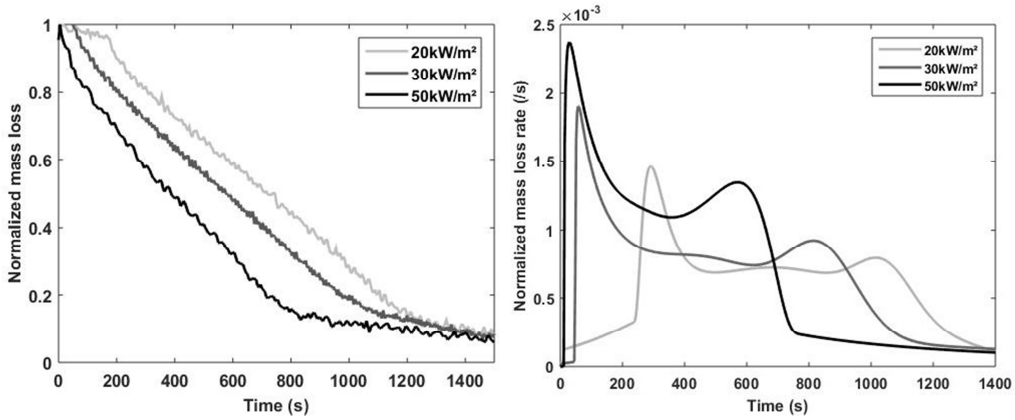

Fig. 3. Experimental cone calorimeter results under air at different heat fluxes: (a) mass loss; (b) mass loss rate.

Similar shapes of the normalized mass loss rate (MLR) are observed for all heat fluxes. Wood is a charring material, therefore a char layer appears above the virgin layer. It explains the decreasing of the MLR after the first peak: the char layer acts as a thermal barrier. The last peak of the mass loss rate is attributed to the heat feedback. This increase of MLR is due to a thermal behavior, the

boundary experimental condition causes a thermal feedback when the thermal wave reaches the back of the sample [18]. From the curves of mass loss, it can be seen a difference of slope when the flame is extinguished. After flame extinguishing, oxygen diffused into the material and oxidized the char residue.

In addition, experimental measurement of the pyrolysis front is made by stopping the test at different times (100, 150, 200, 400, 600 and 700s after the beginning of the experiment), cutting the sample, and measuring the distance between the pyrolysis zone and the bottom of the sample. The pyrolysis front is measured close to the middle of the sample, based on [19]:

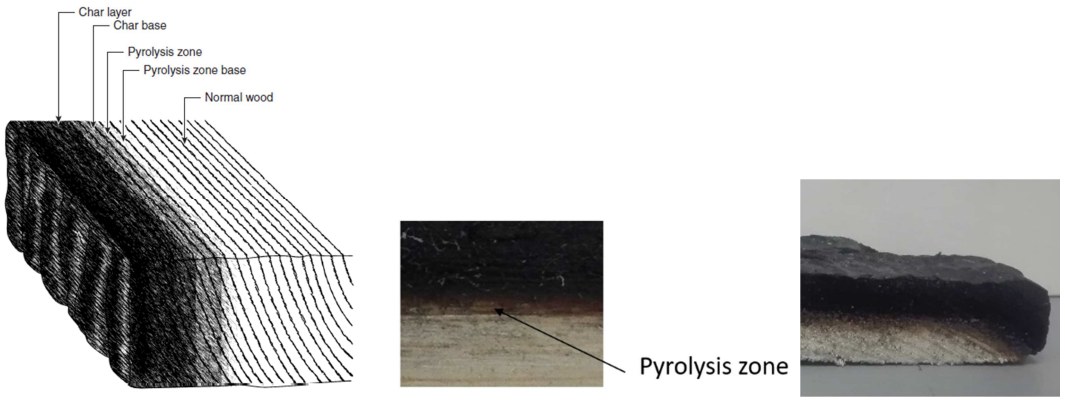

Fig. 4. Pyrolysis zone in a wood section: (a) from [19]; (b) current study; (c) pyrolysis front inhomogeneity (30 kW/m² at 600 s);

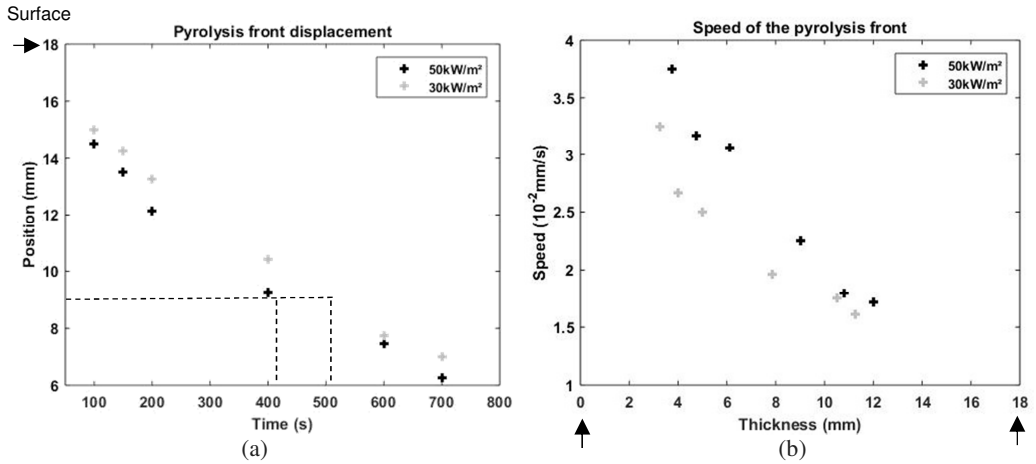

Fig. 5. Experimental result for the pyrolysis front: (a) position of the pyrolysis front; (b) speed of the pyrolysis front along the thickness.

The thickness between the char layer and the virgin layer is very thin (Fig. 4(b)), leading to an accurate measurement of the pyrolysis front. However, it can be seen from the Fig. 4(c) that the pyrolysis front is not linear close to the side. This is due to a slight contraction of the material during the experiment, allowing the incident heat flux to pass through the sides. From the value obtained, the position of pyrolysis front versus time is tracked, as well as the speed of this front along the thickness of the material.

The pyrolysis front reaches the middle of the thickness at 415 s for 50 kW/m² and 510 s for 30 kW/m² (values obtained by polynomial interpolation). Knowing this time, the pyrolysis temperature can be estimated based on the temperature measurement at the middle of the thickness. From Fig. 5(b), the speed of the pyrolysis front decreases, as the char plays a heat barrier.

To finish, experimental investigations for the measurement of the temperature are made for two heat fluxes: 30 and 50 kW/m². The temperatures at 3 mm below the surface exposed, at the middle of the thickness, at the bottom of the sample and 1 cm below the back face (in the sample holder) are recorded using thermocouples of 0.5 mm diameter and of type K. The thermocouples are placed perpendicular to the surface exposed, and closed to the middle. At least seven experiments are performed per heat flux (only one for the 3 mm below the surface at 50 kW/m²). Figure 4 presents the results.

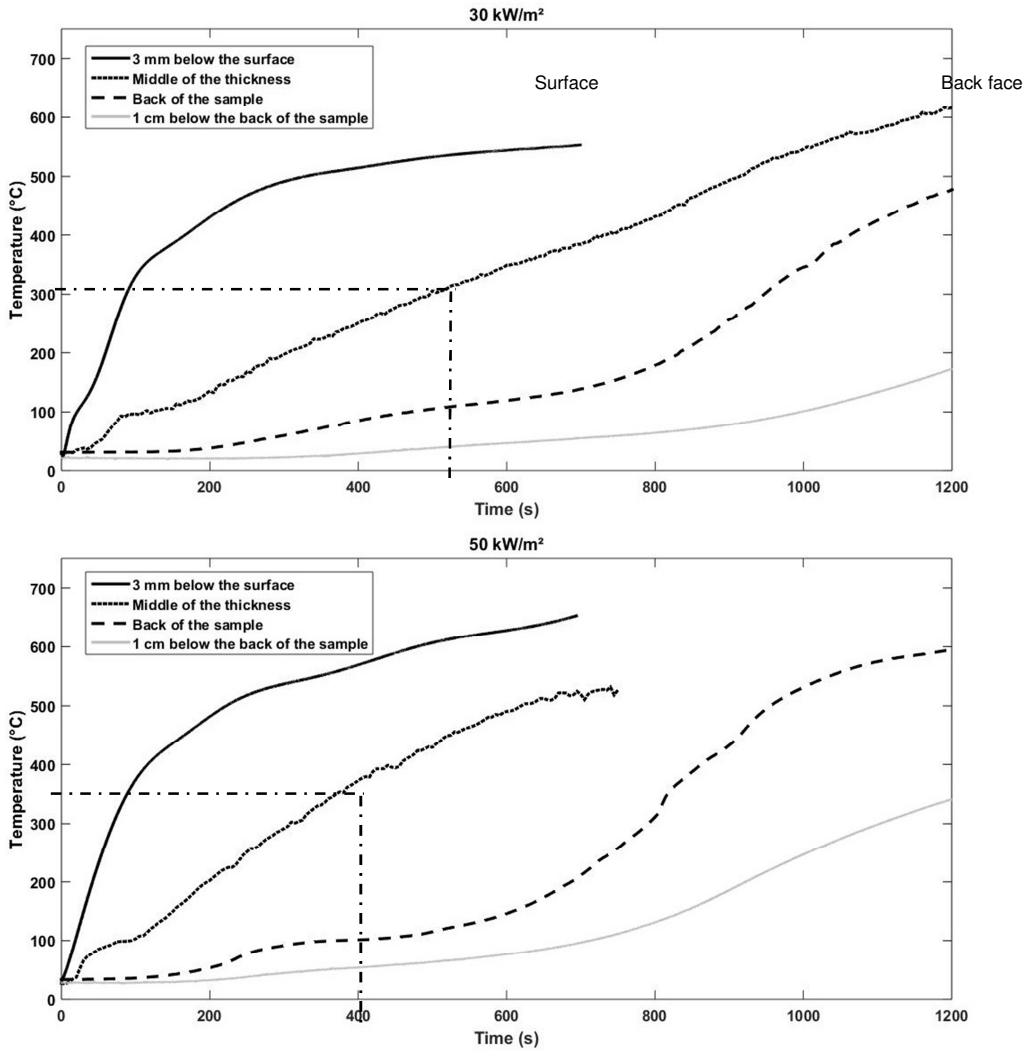

Fig. 6. Experimental temperature for 30 kW/m² and 50 kW/m².

For the 3 mm below to the surface temperature, and for the middle of the sample temperature at 50 kW/m², the results are presented up to 700 s, beyond this value, experimental discrepancies

appear due to the physical change of the wood. The middle of the thickness temperature is used in order to estimate the pyrolysis temperature (dash-dot lines in the middle of the thickness temperature curves). For 50 kW/m², at 415 s, it is found that the temperature is 365 °C, and for 30 kW/m², at 510 s, the temperature is 310 °C. The discrepancy between the two pyrolysis temperatures can be due to the difference in the heating rate when the pyrolysis front reaches the middle of the sample. It can also be due to the discrepancy during the temperature measurement (maximum of 60 °C of standard deviation on the tests). From Fig. 6, the effect of the water evaporation is visible (constant evolution of temperature at around 100 °C). This is more visible in depth of the material. The fact that the water evaporation is more visible at the back of the sample is not due to a slowing down of the thermal wave (as the slopes of the curve of the middle of the thickness and of the back of the sample temperature are quite similar after water evaporation). It can be explained by the presence of water in the sample holder.

Knowing the pyrolysis temperature for each heat flux, the position (and the speed) of the pyrolysis front at 3 mm below the surface and at the back of the sample can be estimated. Figure 7 combines the measured (by cutting the sample) and estimated (by the temperature) position of the pyrolysis front.

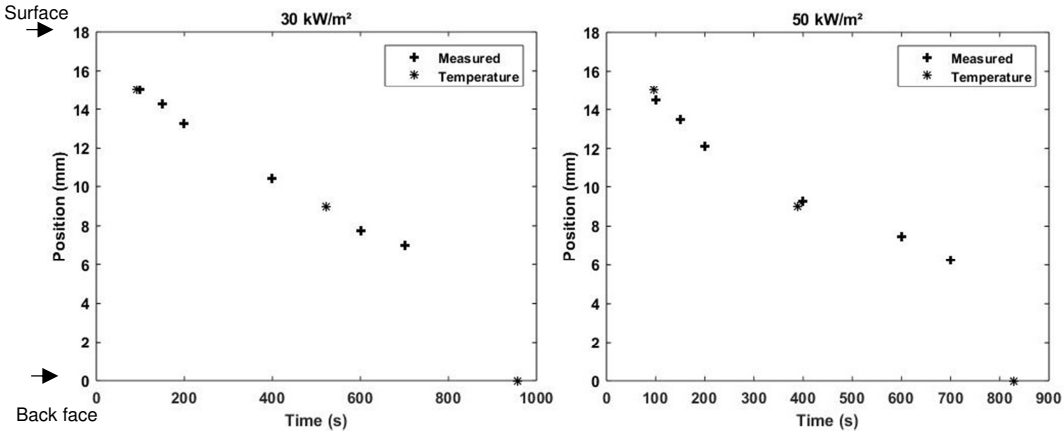

Fig. 7. Experimental position of the pyrolysis front (measured and estimated) for 30kW/m² (a) and 50 kW/m² (b).

The measured and the estimated (with temperature) position of the pyrolysis front appears to be in quite good agreement. The pyrolysis front seems to accelerate close to the back of the sample; this is explained by the thermal feedback caused by the insulated sample holder.

CONE CALORIMETER NUMERICAL RESULTS

Numerical investigations are performed using Fire Dynamic Simulator in order to validate thermochemical properties. Heat transfer is treated in one dimension, and the equation solved is as follows, based on the component-averaged thermal properties:

$$\rho_s c_{P,s} \frac{\partial T_s}{\partial t} = \frac{\partial}{\partial x}\left(\lambda_s \frac{\partial T_s}{\partial x}\right) + \dot{q}'''_{s,c}\,, \tag{3}$$

where $\dot{q}'''_{s,c}$ is the chemical source term. More information can be found in [6]. The overall domain is 30 x 30 x 40 cm^3, with a uniform gas phase mesh of size 1 cm. During the simulations, the lateral

faces are insulated (adiabatic conditions) and an insulated material is placed at the bottom of the sample, which thermal conductivity, heat capacity and density are 0.08 W/(m·K), 1.04 kJ/(kg·K) and 240 kg/m^3, respectively. A uniform mesh is generated for the solid phase (0.5 mm), in order to represent accurately the thermal wave. The Eddy Dissipation Concept is used as a combustion model, the fuel is assumed to be the elementary formula of wood $C_{3.4}H_{6.2}O_{2.5}$, with an effective heat of combustion of 14 MJ/kg, a soot fraction of 0.004 kg/kg and a CO fraction of 0.01 kg/kg. Oxygen diffusion in the sample is taken into account with

$$X_{O_2}(x) = X_{O_2,g} \exp(-x/L), \tag{4}$$

where $X_{O_2,g}$ and $X_{O_2}(x)$ are, respectively, the first gas phase cell oxygen concentration (above the solid), and the in depth oxygen concentration into the sample, L is the maximum length of oxygen penetration in the sample, assumed to be 1 mm. Only the shrinkage of the char reaction is represented.

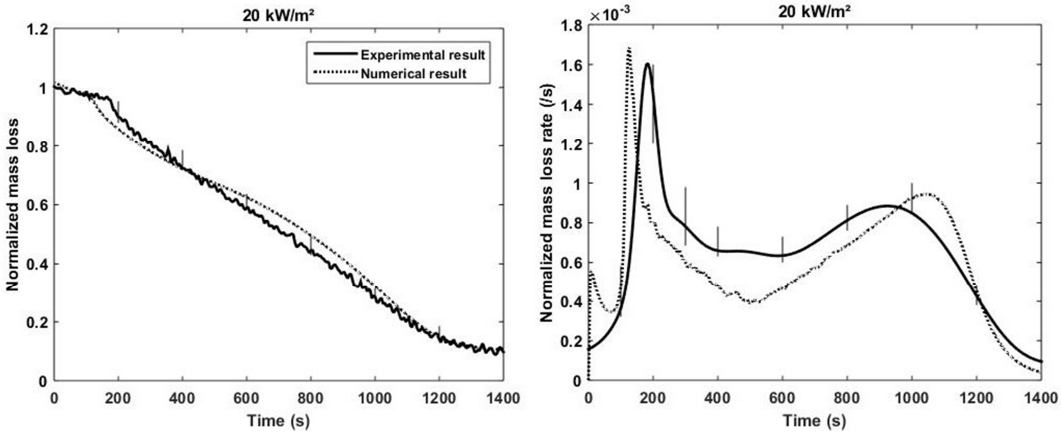

(a) (b)

Fig. 8. Experimental and numerical results at 20 kW/m²: (a) mass loss; (b) mass loss rate.

Mass loss and mass loss rate are presented in the Figs. 8, 9 and 10. Numerical results present a quite good agreement with experimental results, especially since the heat flux is high. However the second peak corresponding to the thermal feedback is over estimated and the steady phase (between the two peaks) is underestimated. This can be explained by the lack of control at the side boundary conditions. As shown in Fig. 4. c, the pyrolysis front reaches the back of the sample first by the side of the sample, which is not taken into account in the simulation. Therefore, between the two peaks, the numerical mass loss rate is slightly underestimated, and the second peak is overestimated. Despite these observations, the simple pyrolysis model can represent the mass loss and the mass loss rate for the three heat fluxes tested.

In addition, the thermal feedback from the insulated condition at the back of the sample is numerically predicated earlier.

Figures 11 and 12 present the comparison between experimental and numerical temperatures. The numerical results can predict correctly the temperature at 3 mm below the surface and at the middle of the thickness (for 50 kW/m², repeatability tests need to be performed). However, the simulations do not predict the temperature at the back of the sample and 1 cm below it, especially around 100 ° C, which can be explained by the presence of water in the sample holder, which is not taken into account in the simulations. The overestimations of the temperature at the back of the face and in the

sample holder explain the fact that the thermal feedback is predicted earlier in the curves of MLR (Figs. 8, 9 and 10).

The final comparison is the pyrolysis front position versus time. Numerically, the pyrolysis front is composed of 50% of wet wood, and 50% of dry wood (270 kg/m^3). Figure 13 compares the numerical and experimental position of the front. For both 30 and 50 kW/m², the pyrolysis front is accurately represented in the simulation. However, when the thermal feedback appears, the front is not correctly estimated, as the temperature at the back of the sample is numerically overestimated.

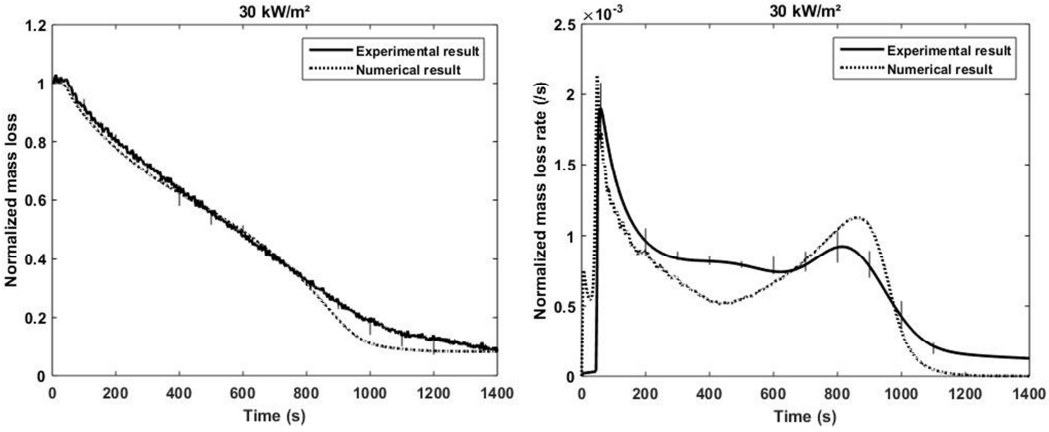

(a) (b)

Fig. 9. Experimental and numerical results at 30 kW/m²: (a) mass loss; (b) mass loss rate.

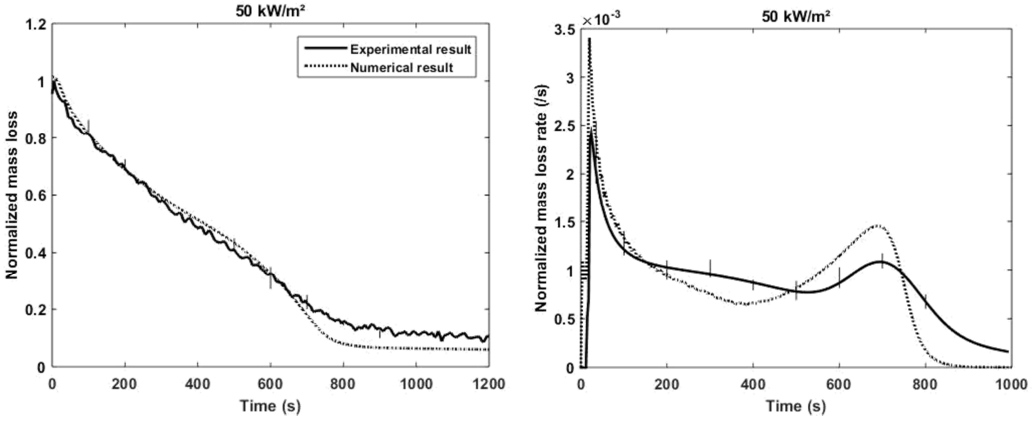

(a) (b)

Fig. 10. Experimental and numerical results at 50 kW/m²: (a) mass loss; (b) mass loss rate.

CONCLUSION

TGA experiments were performed under air and nitrogen at 5 K/min in order to define a model of thermal decomposition. A simple model was defined and kinetic parameters were obtained with a particle swarms optimization. In addition, heat capacity and heat of reaction were determined using the TGA-DSC apparatus. Thermal conductivity of the virgin wood was measured at room temperature with a Modified Transient Plane Source technique (MTPS). Other values of thermal conductivities are taken from the literature, as well as the densities. These parameters serve as input

data for numerical models at cone calorimeter scale. Cone calorimeter experiments were performed with mass loss, mass loss rate, temperature, and pyrolysis front being recorded. The experimental and numerical results are in good agreement. The observed discrepancies are mainly explained by the lack of control of the side boundary conditions: the sides are not insulated, leading to an advanced thermal decomposition at this location. In addition, the presence of water in the sample holder can explain the discrepancies concerning the temperature at the back of the sample and 1 cm below it, as the water evaporation is not simulated in the sample holder. The overestimation of these temperatures leads to the earlier prediction of the thermal feedback and explains the fact that the numerical pyrolysis front reaches the rear face before the experiment.

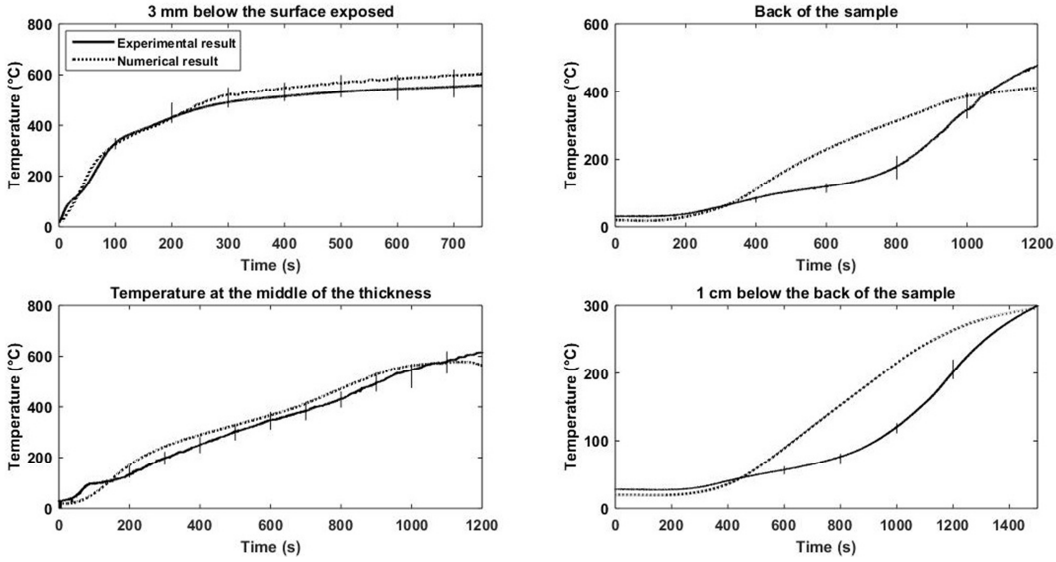

Fig. 11. Experimental and numerical results for temperatures at 30 kW/m²

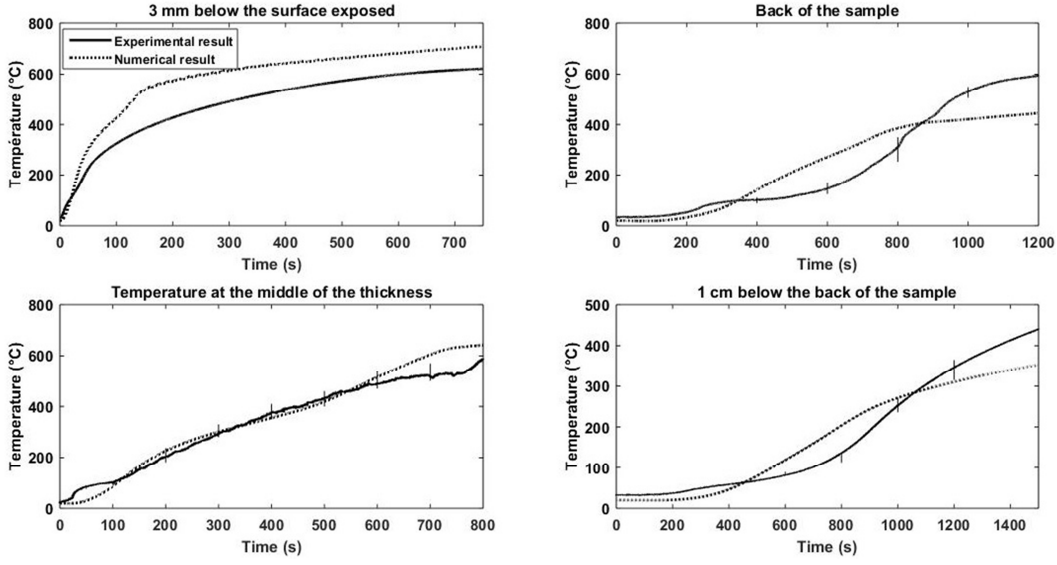

Fig. 12. Experimental and numerical results for temperatures at 50 kW/m².

The thermochemical parameters can represent the thermal behavior of the material. These input parameters can be extrapolated to the next scale of the study: LIFT apparatus for one dimensional lateral flame propagation and radiant panel for one dimensional vertical flame propagation.

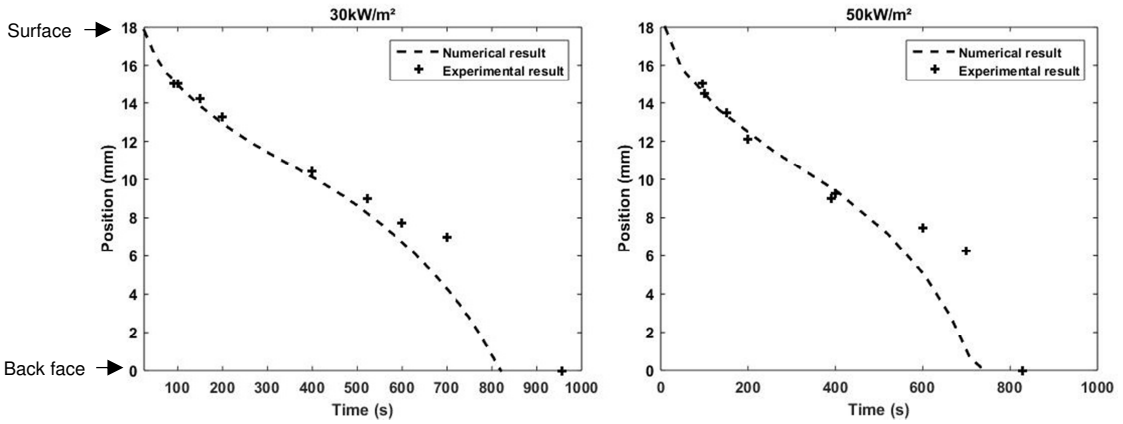

Fig. 13. Experimental and numerical comparison of the pyrolysis front at 30 kW/ (a), and 50 kW /m² (b).

REFERENCES

[1] A. Meunders et al. Parmeter optimization and sensitivity analysis for fire spread modelling with FDS, University of Canterbury, 2014

[2] K. Prasad et al. Numerical simulation of fire spread on polyurethane foam slabs, Proceedings of the Fire and Materials conference, San Francisco, 2009.

[3] J.G. Quintiere, D.W.I. Rouson. Application of CFD Modelling to room fire growth on walls, NIST GCR 03-849, April 2003.

[4] E. Markus, A. Snegirev, E. Kuznetsov, L. Tanklevskiy. Application of the thermal pyrolysis model to predict flame spread over continuous and discrete fire load, Fire Saf. J. (2019).

[5] NIST, Fire Dynamics Simulator User's Guide Sixth Edition – Version 6.6.0

[6] T. Rogaume, et al. Developement of the thermal decomposition mechanism of the polyether polyurethane foam using both condensed and gas phase release data. Combust. Sci. Technol. 627-644 (2011).

[7] D. Marquis, M. Pavageau, E. Guillaume. Multi-scale simulations of fire growth on a sandwich composite structure, J. Fire Sci. 31 (2013) 3-34.

[8] E. Guillaume, A. Camillo, T. Rogaume, Application and limitations of a method based on pyrolysis models to simulate railway rolling stock fire scenarios, Fire Technol. 50 (2014) 317–348.

[9] T. Fateh, F. Richard, T. Rogaume. Modeling of the Pyrolysis of Plywood Exposed to Heat Fluxes under Cone Calorimeter In: D. Nilsson, P. van Hees, R. Jansson. (Ed.), Fire Safety Science–Proceedings of the Eleventh International Symposium, pp, 208-221, 2017.

[10] C. Di Blasi, Modelling chemical and physical processes of wood and biomass pyrolysis, Progr. Energy Combust. Sci. 34 (2008) 47-90.

[11] M. A. Kanury, Thermal decomposition kinetics of wood pyrolysis, Combust. Flame 18 (1972) 75-83.

[12] E. Elbeltagi, T. Hegazy, D. Grierson, Comparison among five evolutionary-based optimization algorithms, Advanced Eng. Inf. 19 (2005) 43-53.

[13] Clerc M. Particle Swarm Optimization. ISTE Ltd, UK, 2006.

[14] S.I. Stoliarov, R.N. Walters, Determination of the heats of gasification of polymers using differential scanning calorimetry, Polymer Degrad. Stab. 93 (2008) 422-427.

[15] J. Li, S.I. Stoliarov, Measurement of kinetics and thermodynamics of the thermal degradation for non-charring polymers, Combust. Flame 160 (2013) 1287-1297.

[16] M. Janssens, Thermo-physical properties of wood for pyrolysis models, Australia, 1994.

[17] M.J. Spearpoint, J.G. Quintiere, Predicting the piloted ignition of wood in the cone calorimeter using an integral model, Combust. Flame 123 (2000) 308-324.

[18] B. Shartel, M. Bartholdi, U. Knoll, Some comments on the use of cone calorimeter data, Polymer Degrad. Stab. 88 (2005) 540–547.

[19] R.H. White, Analytical Methods for determining fire resistance of timber members, In: SFPE Handbook of Fire Protection Engineering, Third Ed., pp. 4-257 – 4-273, NFPA, 2002.